

Supersymmetric effects in top quark decay into polarized W-boson

Junjie Cao ^{a,b}, Robert J. Oakes ^c, Fei Wang ^b and Jin Min Yang ^b

^a Department of Physics, Henan Normal University, Xinxiang, Henan 453002, China

^b Institute of Theoretical Physics, Academia Sinica, Beijing 100080, China

^c Department of Physics and Astronomy, Northwestern University, Evanston, IL 60208, USA

(May 22, 2019)

We investigate the one-loop supersymmetric QCD (SUSY-QCD) and electroweak (SUSY-EW) corrections to the top quark decay into a b -quark and a longitudinal or transverse W -boson. The corrections are presented in terms of the longitudinal ratio $\Gamma(t \rightarrow W_L b)/\Gamma(t \rightarrow W b)$ and the transverse ratio $\Gamma(t \rightarrow W_{\pm} b)/\Gamma(t \rightarrow W b)$. In most of the parameter space, both SUSY-QCD and SUSY-EW corrections to these ratios are found to be less than 1% in magnitude and they tend to have opposite signs. The corrections to the total width $\Gamma(t \rightarrow W b)$ are also presented for comparison with the existing results in the literature. We find that our SUSY-EW corrections to the total width differ significantly with previous studies: the previous studies give a large correction of more than 10% in magnitude for a large part of the parameter space while our results reach only few percent at most.

14.65.Ha 12.60.Jv 11.30.Pb

I. INTRODUCTION

As the most massive fermion in the Standard Model (SM), top quark is believed to be sensitive to new physics [1]. Since the measurements of top quark properties in Run 1 at the Fermilab Tevatron have only small statistics, there remains plenty of room for new physics to be discovered in future precision measurements. Such possibilities exist on our horizon: while the upgraded Tevatron collider will significantly improve the precision of the top quark measurements, the CERN Large Hadron Collider (LHC) and the planned Next-generation Linear Collider (NLC) will serve as top quark factories and allow precision measurements of the top quark properties [2].

Although various exotic production processes [3] and rare decay modes [4] of the top quark will serve as robust evidence of new physics (since these exotic processes are forbidden or severely suppressed in the SM), the role of the dominant decay mode $t \rightarrow W b$ in probing new physics should not be underestimated [5]. One advantage of this decay mode is that it is free of non-perturbative theoretical uncertainties [6] and thus future precision experimental data can be compared with accurate theoretical predictions. The other advantage of this channel is that the decay product W -boson is strongly polarized and the helicity contents (transverse-plus W_+ , transverse-minus W_- and longitudinal W_L) of the W -boson can be probed through a measurement of the shape of the lepton spectrum in the W -boson decay [7]. Therefore, the study of top decay into a polarized W -boson will provide additional information about tWb coupling ¹ and has so far attracted a lot of attention from both theorists and experimentalists. On the experimental side, the CDF collaboration has already performed the measurement of the helicity component of the W -boson in top quark decay from Run 1 data and obtained the results

$$\begin{aligned}\Gamma_L/\Gamma &= 0.91 \pm 0.37(stat.) \pm 0.13(syst.), \\ \Gamma_+/\Gamma &= 0.11 \pm 0.15 ,\end{aligned}$$

where Γ is the total decay rate of $t \rightarrow W b$, and Γ_L and Γ_+ denote respectively the rates into a longitudinal and transverse-plus W -boson. Although the error of these measurements is quite large at the present time, it is expected to be reduced significantly during Run 2 of the Tevatron and may reach 1% \sim 2% at the LHC [8]. On the theoretical side, predictions of these quantities in the SM up to one-loop level are now available. The tree-level results are 0.703 for Γ_L/Γ , 0.297 for Γ_-/Γ and $\mathcal{O}(10^{-4})$ for Γ_+/Γ . The QCD corrections to these predictions are respectively -1.06% , 2.17% and 0.10% [9], while the electroweak corrections are at the level of a few permill [10].

¹Among the three polarizations of the W -boson in top decay, the longitudinal mode is of particular interest since it is relevant for the understanding of the electroweak symmetry breaking mechanism.

In order to probe new physics from the future precise measurement of Γ_L/Γ , Γ_-/Γ or Γ_+/Γ , we must know the new physics contributions to these quantities in various models. In this article we focus on the supersymmetric contributions in the framework of the Minimal Supersymmetric Model (MSSM). In this model the one-loop corrections to the total width of $t \rightarrow bW$ have been studied by several groups [11–15]. However, the corrections to Γ_L/Γ , Γ_-/Γ or Γ_+/Γ are still lacking and calculating these corrections is the major goal of this article.

In the MSSM the genuine supersymmetric corrections (i.e., the corrections from various sparticle loops) are SUSY electroweak (SUSY-EW) corrections, arising from interactions of charginos or neutralinos, and SUSY-QCD corrections, arising from interactions of gluinos². The SUSY-EW and SUSY-QCD corrections to the total width were first investigated in [11,12] without considering squark mixings, and later were restudied extensively in [13–15] by taking into account the squark mixings. Although our aim in this paper is to study the corrections to Γ_L/Γ , Γ_-/Γ and Γ_+/Γ , we will also repeat the calculations of the corrections to the total width for two reasons: One is that the previous SUSY-EW calculations were performed many years ago and some SUSY parameter space viable at that time has been ruled out by recent experiments. The other reason is that the SUSY-EW corrections to the total width were found to be exceptionally large (exceeds 10% in a large part of parameter space) [13] and should, therefore, be checked carefully. In fact we find they are much smaller for reasons we will discuss.

This paper is organized as follows. In section II, we present relevant formula for our calculations. In section III, SUSY-EW corrections are calculated and compared with previous studies. In section IV, we examine SUSY-QCD corrections. For the numerical calculations of both SUSY-EW and SUSY-QCD corrections, we first perform a scan in the typical allowed parameter space to find out the typical size of the corrections, and then consider some special scenarios (such as a very light sbottom or gluino) to figure out if the corrections are exceptionally large in some regions of parameter space. The conclusions are given in section V.

II. FORMALISM

In this section we present the formulas for calculating new physics contributions to $t \rightarrow bW$ in the so-called “ G_F -scheme”, which is actually the usual on-shell scheme [17] by choosing the Fermi constant G_F and the pole masses m_W , m_t , m_b , \dots , as input parameters. These formulas are valid for studying one-loop corrections to the decay $t \rightarrow Wb$ in any renormalizable new physics model.

The tWb vertex at one-loop level takes the form [17]

$$\Gamma_\mu = -i2^{3/4}G_F^{1/2}m_W V_{tb} \left\{ \gamma_\mu P_L \left(1 + \frac{1}{2}\delta Z_b^L + \frac{1}{2}\delta Z_t^L + \delta Z_1^W - \delta Z_2^W - \frac{1}{2}\Pi_W - \frac{1}{2}\Delta r^{\text{new}} + F_L \right) + \gamma_\mu P_R F_R + p_{t\mu} P_L H_L + p_{t\mu} P_R H_R \right\}. \quad (1)$$

Here $P_{R,L} \equiv \frac{1}{2}(1 \pm \gamma_5)$ are the chirality projectors. The form factors $F_{L,R}$ and $H_{L,R}$ represent the contributions from irreducible vertex loops. Δr^{new} is the corresponding new physics contribution to Δr . δZ_b^L and δZ_t^L denote respectively the field renormalization constant for bottom quark and top quark. Π_W and $\delta Z_{1,2}^W$ are related to the renormalization of the W -boson and their expressions in terms of the self-energies of gauge bosons are given explicitly in [17].

By decomposing Δr^{new} into the universal part and non-universal part, i.e., $\Delta r^{\text{new}} = \Delta r_U^{\text{new}} + \Delta r_{NU}^{\text{new}}$, and inserting the explicit forms of $\delta Z_{1,2}^W$, one can re-express Γ_μ as [17]

$$\Gamma_\mu = -i2^{3/4}G_F^{1/2}m_W V_{tb} \left\{ \gamma_\mu P_L \left(1 + \frac{1}{2}\delta Z_b^L + \frac{1}{2}\delta Z_t^L - \frac{1}{c_W s_W} \frac{\Sigma_{\gamma Z}(0)}{m_Z^2} - \frac{1}{2}\Sigma'_W(m_W^2) - \frac{1}{2} \frac{\Sigma_W(0) - \delta m_W^2}{m_W^2} - \frac{1}{2}\Delta r_{NU}^{\text{new}} + F_L \right) + \gamma_\mu P_R F_R + p_{t\mu} P_L H_L + p_{t\mu} P_R H_R \right\}, \quad (2)$$

where $c_W = \cos\theta_W$, $s_W = \sin\theta_W$, $\Sigma_{\gamma Z}(0)$ is the new physics contribution to unrenormalized γ - Z transfer at zero momentum and Σ_W is the new physics effect on the W -boson self-energy.

²The corrections from the Higgs interactions to the total width of $t \rightarrow bW$ are not unique to the MSSM since they also exist in the general two-Higgs-doublet models. Such corrections are found to be less than 1% for the whole parameter space [16]. Therefore we do not calculate such corrections in this paper.

In our calculations we adopted all the conventions in [17] except for the fermion-field renormalization. To be valid in general cases, the self-energy of a fermion is decomposed as

$$\Sigma_f(p) = \Sigma_f^L(p^2) \not{p} P_L + \Sigma_f^R(p^2) \not{p} P_R + m_f \Sigma_f^{SL}(p^2) P_L + m_f \Sigma_f^{SR}(p^2) P_R. \quad (3)$$

Using the on-shell conditions for external fermion fields [18], we obtain δZ_f as

$$\delta Z_f^L = \tilde{\Sigma}_f^L(m_f^2) + m_f^2 \left[\tilde{\Sigma}_f^{L'}(m_f^2) + \tilde{\Sigma}_f^{R'}(m_f^2) + \tilde{\Sigma}_f^{SL'}(m_f^2) + \tilde{\Sigma}_f^{SR'}(m_f^2) \right], \quad (4)$$

$$\delta Z_f^R = \tilde{\Sigma}_f^R(m_f^2) + m_f^2 \left[\tilde{\Sigma}_f^{L'}(m_f^2) + \tilde{\Sigma}_f^{R'}(m_f^2) + \tilde{\Sigma}_f^{SL'}(m_f^2) + \tilde{\Sigma}_f^{SR'}(m_f^2) \right], \quad (5)$$

where $\tilde{\Sigma}$ means to take the real part of the loop integrals but not of the coupling constants in the fermion self-energies and $\tilde{\Sigma}' \equiv \partial \tilde{\Sigma} / \partial p^2$.

The rate of the top decay into a polarized W -boson can be obtained by using the explicit expression of polarization vector of W -boson³ or using the project technique introduced in [9,10]. Through some tedious calculations we obtain

$$\Gamma_L = \frac{G_F m_W^2 m_t |V_{tb}|^2 (1-x^2)^2}{8\sqrt{2}\pi x^2} \left\{ 1 + \text{Re}(\delta Z_b^L + \delta Z_t^L + 2\delta Z_1^W - 2\delta Z_2^W - \Pi_W - \Delta r^{new} + 2F_L) \right. \\ \left. + \text{Re}(H_R) m_t (1-x^2) \right\}, \quad (6)$$

$$\Gamma_- = \frac{G_F m_W^2 m_t |V_{tb}|^2}{8\sqrt{2}\pi} (1-x^2)^2 2 \left\{ 1 + \text{Re}(\delta Z_b^L + \delta Z_t^L + 2\delta Z_1^W - 2\delta Z_2^W - \Pi_W - \Delta r^{new} + 2F_L) \right\}, \quad (7)$$

where Γ_L (Γ_-) denotes the rate of top decay into longitudinal (transverse-minus) W -boson and $x = m_W/m_t$. In deriving Eqs.(6,7) we have neglected b -quark mass for simplicity and this will introduce an uncertainty of several permillage on $\Gamma_{L,-}$. Another consequence of neglecting m_b is $\Gamma_+ = 0$ due to angular momentum conservation [9] and, as a result, the total decay rate of $t \rightarrow bW$ is obtained by $\Gamma = \Gamma_L + \Gamma_-$. In our following calculations, we retain the bottom quark mass only when it appears in couplings or in sbottom mass matrix [19] since in those cases the bottom quark mass is multiplied by $\tan\beta$ and can not be neglected for large $\tan\beta$.

We define the ratios

$$\hat{\Gamma}_{L,-} = \Gamma_{L,-} / \Gamma, \quad (8)$$

which can be measured in experiments. In our numerical results we will present the relative SUSY corrections to them, i.e., $\delta \hat{\Gamma}_{L,-} / \hat{\Gamma}_{L,-}^0$ with $\delta \hat{\Gamma}_{L,-}$ denoting the SUSY corrections and $\hat{\Gamma}_{L,-}^0$ denoting the SM predictions.

III. SUSY ELECTROWEAK CORRECTIONS

Now we concentrate on SUSY electroweak corrections. First we consider vertex corrections and quark self-energy corrections as depicted in Fig. 1. This part of the corrections are expected to be sizable for large $\tan\beta$. In Appendix A, we list in detail the relevant Feynman rules and present our analytical results. We checked that our results do reduce to those in [11] when switching off squark mixings and neglecting the b -quark mass in quark-squark-chargino (or neutralino) interactions.

The SUSY-EW contributions to the self-energies of gauge bosons, which are necessary to calculate for $\delta Z_{1,2}^W$ and Π_W , have been calculated by several groups [11,20]. We recalculated them and find that our results agree with those in [11] when switching off squark mixings. In our numerical calculations we will take into account the mixings between top-squarks and between sbottoms.

As to the SUSY-EW contributions to Δr , both the universal and non-universal parts are nicely presented in [21]. We checked the analytic expressions and incorporated them in our fortran code. Our numerical results show that the total contribution to the width $\Gamma(t \rightarrow Wb)$ from $\delta Z_{1,2}^W$, Π_W and $\Delta r^{\text{SUSY-EW}}$ is generally less than 1%.

³For the construction of covariant polarization vector of W -boson, see Eq.(5.16) in [18].

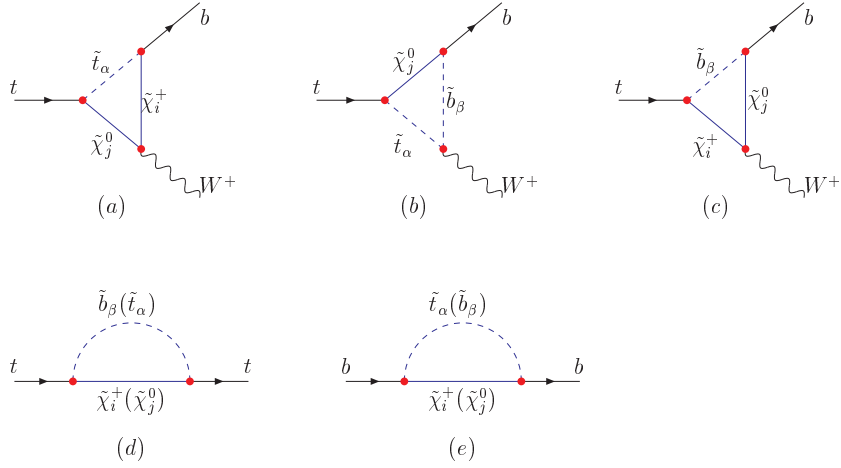


FIG. 1. Some of the Feynman diagrams of SUSY-EW corrections to $t \rightarrow Wb$: (a-c) are vertex loops; (d,e) are top and bottom quark self-energy loops.

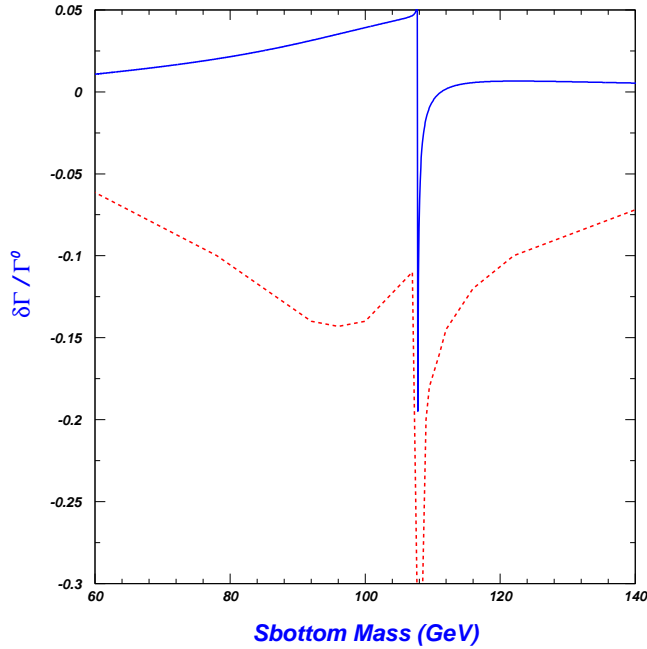


FIG. 2. SUSY electroweak corrections to the width $\Gamma(t \rightarrow Wb)$ versus sbottom mass. Solid curve is our result and the dashed curve is taken from Fig. 7 of Ref.[13]. The input parameters are those of case C in Fig. 7 in Ref.[13].

As pointed out in Appendix A, our vertex corrections are quite different from those in [13]. To see the numerical difference between our results and those in [13], we present a comparison in Fig. 2, which corresponds to the case C of Fig. 7 in [13]. We see from Fig. 2 that the difference is significant. The results of [13] are much larger in magnitude than ours: in a large part of parameter space the results of [13] exceed 10% in size while our results are below 5%.

Fig. 2 also shows for both results a common feature, namely, there exists a peak in the correction at $m_{\tilde{b}} \simeq 109$ GeV. This peak is from the “threshold effect” [22], which is explained in Appendix B.

Note that some of the input parameters in Fig. 2, which were allowed at the time when the calculations in [13] were performed, may no longer be allowed nowadays. In our following numerical calculations, we will consider the current constraints on the parameters.

The relevant SUSY parameters in our calculations are: (1) $\tan\beta$, \tilde{M}_Q , \tilde{M}_U , \tilde{M}_D , μ and $A_{t,b}$ which enter mass matrices of top-squark and sbottom [19] (see Appendix A); (2) soft-breaking gaugino masses \tilde{M}_1 and \tilde{M}_2 appearing

in chargino and neutralino mass matrices (see Appendix A); (3) the masses of sleptons and the first two generation squarks involved in the calculation of $\delta Z_{1,2}^W$, Π_W and $\Delta r^{\text{SUSY-EW}}$. To lessen the number of parameters our results depend on, we assume an universal soft breaking parameter \tilde{M}_L and neglect left-right mixings for sleptons and the first two generation squarks. Such assumptions do not affect our numerical results significantly since, as we said before, the contributions from $\delta Z_{1,2}^W$, Π_W and Δr^{new} are small for the allowed parameter space. As for soft breaking gaugino mass parameters \tilde{M}_1 and \tilde{M}_2 , we assume the relation $\tilde{M}_1 \simeq 0.5\tilde{M}_2$ [23]. With these assumptions the relevant SUSY parameters are reduce to

$$\tilde{m}_Q, \tilde{m}_U, \tilde{m}_D, A_t, A_b, \mu, \tan \beta, \tilde{M}_L, \tilde{M}_2. \quad (9)$$

To estimate the size of the SUSY-EW effects, we first performed a scan over the nine parameters in Eq. (9). In our scan we restricted the parameters with mass dimensions to be less than 1 TeV and considered the following experimental constraints:

- (1) $\mu > 0$ and a large $\tan \beta$ in the range $5 \leq \tan \beta \leq 70$, which seems favored by the muon $g - 2$ measurement [24].
- (2) $\delta \rho < 0.002$ [25], which will constrain the mass splitting between stops and sbottoms⁴.
- (3) The LEP and CDF lower mass bounds on sparticles and the lightest CP-even Higgs boson [25,27]

$$\begin{aligned} m_{\tilde{t}} &\geq 86.4 \text{ GeV}, \quad m_{\tilde{b}} \geq 75.0 \text{ GeV}, \quad m_{\tilde{\chi}^+} \geq 67.7 \text{ GeV}, \quad m_{\tilde{\chi}^0} \geq 40 \text{ GeV}, \\ m_{\tilde{\tau}} &\geq 95 \text{ GeV}, \quad m_{\tilde{\nu}} \geq 41 \text{ GeV}, \quad m_{\tilde{q}} \geq 138 \text{ GeV}, \quad m_{h^0} \geq 91 \text{ GeV}, \end{aligned} \quad (10)$$

where $m_{\tilde{q}}$ denotes the mass of squarks of the first two generations.

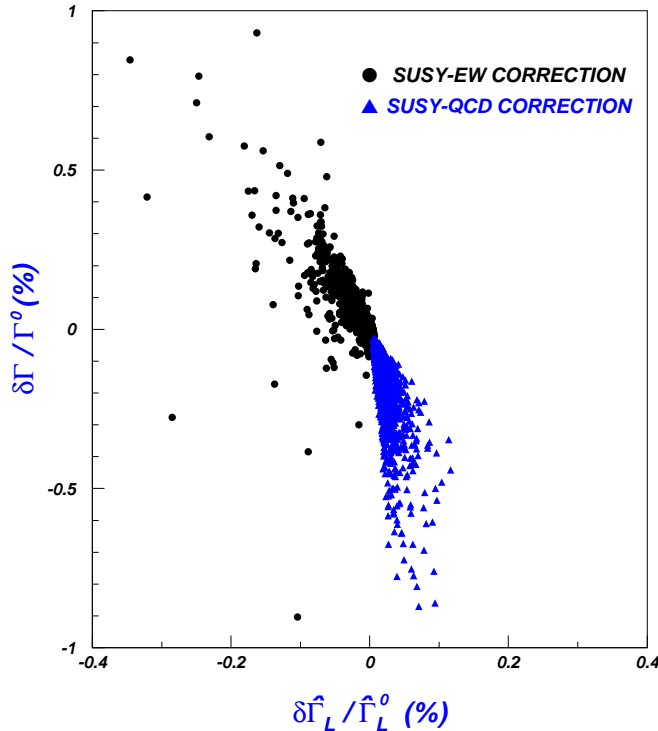


FIG. 3. The scattered plot in the plane of $\delta\Gamma/\Gamma^0$ versus $\delta\hat{\Gamma}_L/\hat{\Gamma}_L^0$.

⁴We use the programme FeynHiggs [26] to generate the values of $\delta\rho$ and Higgs masses.

Our scan results are shown in Fig. 3 in the plane of $\delta\Gamma/\Gamma^0$ versus $\delta\hat{\Gamma}_L/\hat{\Gamma}_L^0$. In our calculations throughout this paper, we have fixed $G_F = 1.16637 \times 10^{-5} \text{ GeV}^{-2}$, $m_W = 80.451 \text{ GeV}$, $m_t = 174.3 \text{ GeV}$ and $m_b = 4.8 \text{ GeV}$. Fig. 3 shows that the SUSY-EW correction is generally below one percent in size and tends to be positive for Γ and negative for $\hat{\Gamma}_L$.

Although the SUSY-EW correction turns out to be quite small (below one percent in size) in the dominant part of the allowed parameter space, we found from our scan that the correction can reach a few percent in some narrow corners of the parameter space. These corners have two feathers: (1) $\mu \ll \tilde{M}_2$ so that the lighter chargino and the lightest neutralino are Higgsino-like, and $\tan\beta$ is large so that the b -quark Yukawa couplings in quark-squark-Higgsino interactions can be greatly enhanced [19]; (2) The two sparticles in a self-energy loop of top quark lie below the threshold, or in other words, the sum of the masses of the two sparticles is lighter than top quark mass. Generally speaking, for $m_{\tilde{b}_1^-} + m_{\tilde{\chi}_1^+} < m_t$ the sbottom(\tilde{b}_1)-chargino($\tilde{\chi}_1^+$) loop can give a relatively large contribution. With the increase of $m_{\tilde{b}_1^-}$ and $m_{\tilde{\chi}_1^+}$, the contributions from this loop decrease as required by a decoupling theorem. A peak in correction size occurs at $m_{\tilde{b}_1^-} + m_{\tilde{\chi}_1^+} = m_t$, as shown in Fig. 2 and explained in Appendix B. To show the size of the corrections in such corners of the parameter space, we present some numerical results in two special scenarios:

- Scenario I: We assume $\mu \ll M_2$ and assume an universal soft-breaking mass M_{SUSY} for squarks.
- Scenario II: We assume a very light sbottom \tilde{b}_1 of about 5 GeV. So far such a light sbottom has not been ruled out by current experiments if the sbottom mixing angle θ_b is tuned to satisfy $\cos\theta_b \simeq 0.38$ [28]. For such a light sbottom, $\tan\beta$ must be large enough to cause a sufficiently large mass splitting between the two sbottom mass eigenstates. In addition, the lighter top-squark \tilde{t}_1 cannot be heavier than 300 GeV in order to satisfy $\delta\rho$ bound.

The results in Scenario I are plotted in Figs. 4 and 5. We present our result only in the region where constraints below Eq.(9) are satisfied. The peaks in these figures happen at $m_{\tilde{b}_1^-} + m_{\tilde{\chi}_1^+} = m_t$ where $m_{\tilde{b}_1^-}$ and $m_{\tilde{\chi}_1^+}$ are the lighter sbottom and top-squark masses, respectively. Fig. 4 shows that below the threshold the SUSY-EW corrections to the width can be as large as 3% for $\tan\beta \geq 50$ and after crossing the threshold, the corrections change sharply to -8% and then quickly decrease in size. About the behavior at threshold, we want to point out that the results within the region $0 \leq m_{\tilde{b}_1^-} + m_{\tilde{\chi}_1^+} - m_t < \Gamma/2$ are not reliable since perturbative expansion of S -matrix element breaks down for these points [13] (also see discussions in Appendix B). Fig. 5 shows that $\delta\hat{\Gamma}_-/\hat{\Gamma}_-^0$ can reach 1% near the threshold and its size is generally larger than that of $\delta\hat{\Gamma}_L/\hat{\Gamma}_L^0$.

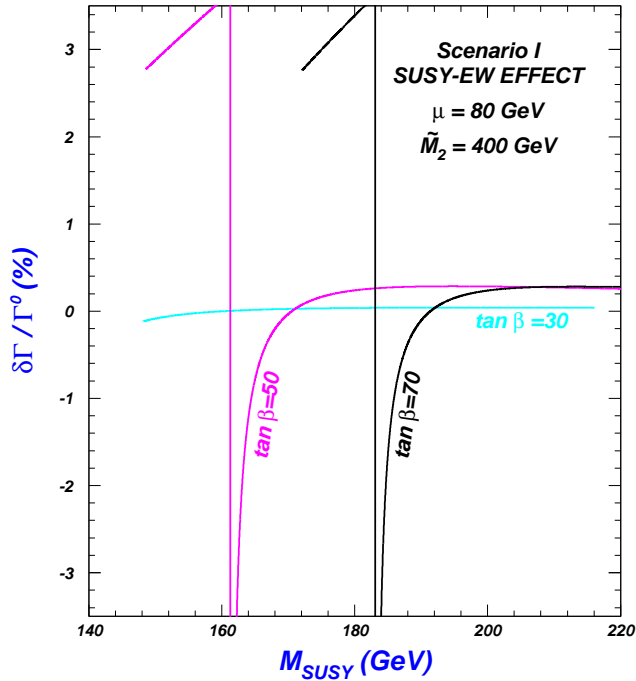


FIG. 4. SUSY electroweak corrections to Γ versus M_{SUSY} in Scenario I.

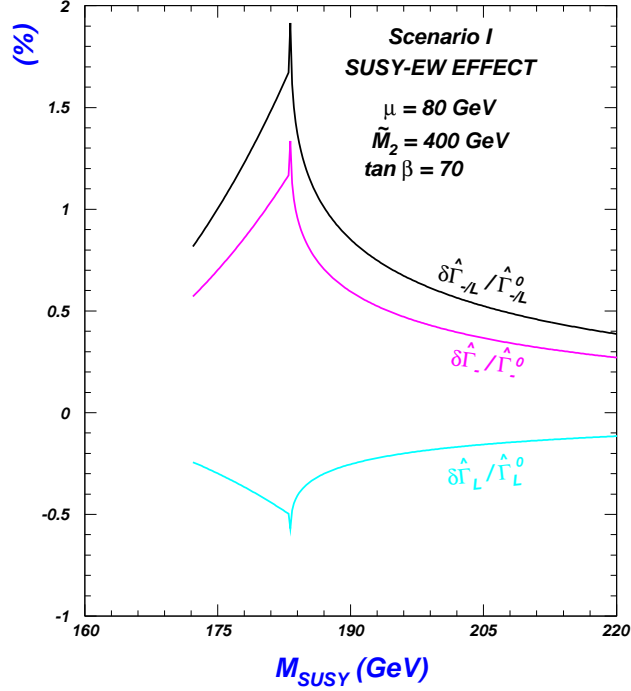


FIG. 5. SUSY electroweak corrections to $\hat{\Gamma}_{-,L}$ and $\hat{\Gamma}_{-/L}(\equiv \hat{\Gamma}_{-}/\hat{\Gamma}_L)$ versus M_{SUSY} in Scenario I.

For numerical calculations in Scenario II, it is inconvenient to take the parameters in Eq.(9) as input. Instead, we may choose

$$m_{\tilde{b}_1}, m_{\tilde{t}_1}, m_{\tilde{t}_2}, \mu, A_b, \theta_b, \tan \beta, \tilde{M}_L, \tilde{M}_2 \quad (11)$$

as input parameters. Using the formula listed in Appendix A, one may relate these two sets of parameters. From our numerical study we found that in this scenario the results are not sensitive to A_b , $m_{\tilde{t}_{1,2}}$ or \tilde{M}_L , and we fix them to be

$$m_{\tilde{t}_1} = 150 \text{ GeV}, m_{\tilde{t}_2} = 500 \text{ GeV}, \tilde{M}_L = A_b = 300 \text{ GeV}. \quad (12)$$

Other parameters are fixed to be

$$m_{\tilde{b}_1} = 5 \text{ GeV}, \quad \cos \theta_b = 0.38, \quad \tilde{M}_2 = 400 \text{ GeV}. \quad (13)$$

The results in Scenario II are plotted in Figs. 6 and 7. In Fig. 6 we plot $\delta\Gamma/\Gamma^0$ versus μ and in Fig. 6 we plot $\delta\hat{\Gamma}_{-,L}/\hat{\Gamma}_{-,L}^0$ and $\delta\hat{\Gamma}_{-/L}/\hat{\Gamma}_{-/L}^0$ versus μ . Again we see that a large $\tan \beta$ can cause large SUSY-EW corrections. Fig. 6 shows a broad region of μ in which corrections to the width can be a few percent. Like in Fig. 4 the peaks occur at $m_{\tilde{b}_1} + m_{\tilde{\chi}_1^+} = m_t$. Fig.7 shows that, like in Scenario I, the SUSY-EW corrections to $\hat{\Gamma}_{-}$ and $\hat{\Gamma}_L$ are of opposite sign and the size of the former is larger than that of the latter.

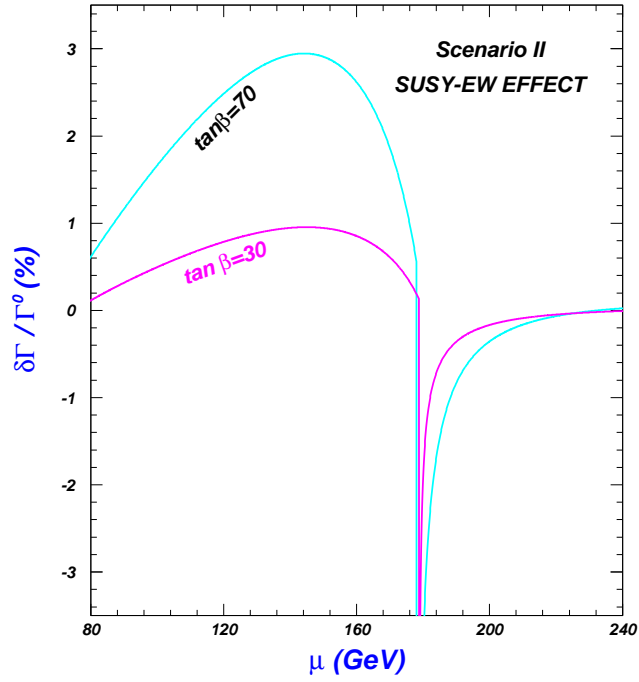


FIG. 6. SUSY electroweak corrections to Γ versus μ in Scenario II.

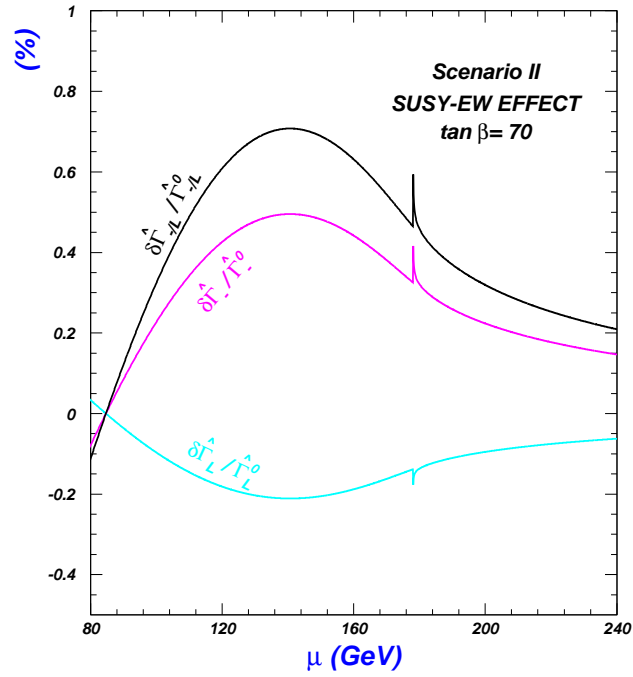


FIG. 7. SUSY electroweak corrections to $\hat{\Gamma}_{-,L}$ and $\hat{\Gamma}_{-/L}$ versus μ in Scenario II.

IV. SUSY-QCD CORRECTIONS

In this section, we investigate SUSY-QCD effects. Compared with SUSY-EW corrections, SUSY-QCD corrections are easier to calculate since $\delta Z_{1,2}^W$, Π_W and δr^{new} receive no contribution from SUSY-QCD interaction at the one-loop level and consequently, one only needs to calculate quark self-energy and vertex correction depicted in Fig. 8.

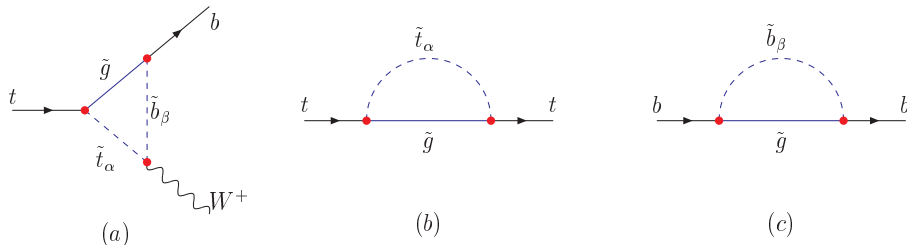


FIG. 8. Feynman diagrams for SUSY-QCD contribution to $t \rightarrow Wb$.

Our analytical results for $F_{L,R}$ and $H_{L,R}$ agree with those in Ref. [14] and thus we do not present our analytic results here. Our numerical results for the corrections to the total width $\Gamma(t \rightarrow Wb)$ agree with Ref. [15] for the same choice of parameters.

The parameters involved in numerical evaluations are gluino mass $m_{\tilde{g}}$, and \tilde{m}_Q , \tilde{m}_U , \tilde{m}_D , A_t , A_b , μ and $\tan \beta$ which enter the mass matrices of top-squark and sbottom [19]. In order to compare the size of SUSY-QCD corrections with that of SUSY-EW corrections, we have shown our scan results of SUSY-QCD corrections in Fig. 3 in the preceding section. In our scan we have considered the relevant constraints listed below Eq.(9) and we also required $m_{\tilde{g}} \geq 200$ GeV, which is the current experimental bound for the gluino in the framework of minimal supergravity model [25]. From Fig. 3 one sees that the SUSY-QCD corrections and SUSY-EW corrections tend to have the opposite signs, and thus they may cancel in large parts of parameter space. This differs drastically from the conclusion of Ref. [13,14] which claims that the two type corrections have the same sign and thus the combined contribution can reduce the width $\Gamma(t \rightarrow Wb)$ by as much as 25%.

We see from Fig. 3 that the SUSY-QCD corrections are smaller than 1% in magnitude in the allowed parameter space with $m_{\tilde{g}} \geq 200$ GeV. However, we found that the corrections can reach a few percent in some corners of the parameter space if we relax the bound $m_{\tilde{g}} \geq 200$ GeV (this bound is model-dependent). In the following we present some numerical results by relaxing this bound $m_{\tilde{g}} \geq 200$ GeV, and in order to compare with SUSY-EW corrections we consider the same two scenarios as in the preceding section.

The results in Scenario I are plotted in Figs. 9 and 10 for different $m_{\tilde{g}}$ values in the allowed region of M_{SUSY} . We fixed $\mu = 80$ GeV and $\tan \beta = 70$, and included the possibility of a very light gluino of 16 GeV, which has not been excluded by current experiments ⁵ (for comparison we also plot a curve with a 100 GeV gluino although it may be severely disfavored by existing experiments). Fig. 9 shows that the magnitude of SUSY-QCD corrections decrease as M_{SUSY} or $m_{\tilde{g}}$ becomes large. Comparing with the SUSY-EW corrections in Fig. 4, one sees the maximum size of the SUSY-QCD corrections is smaller than that of the SUSY-EW corrections, which can be greatly enhanced by b -quark Yukawa coupling for a large $\tan \beta$.

⁵Such a very light gluino has not been excluded by experiments and was recently used to solve the long-standing b -quark production puzzle [29]. To do that, a light sbottom of about 5 GeV is also required, which leads to a stronger constraint from R_b on the SUSY parameters [30].

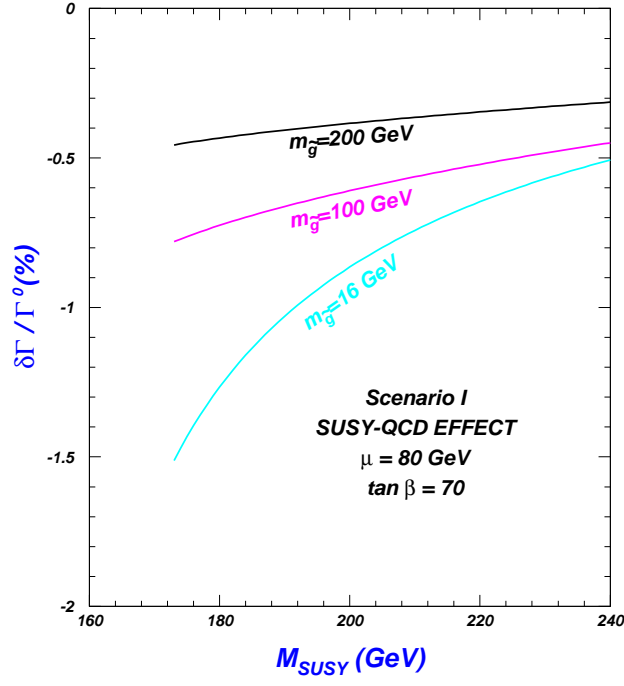


FIG. 9. SUSY-QCD correction to Γ versus M_{SUSY} in Scenario I.

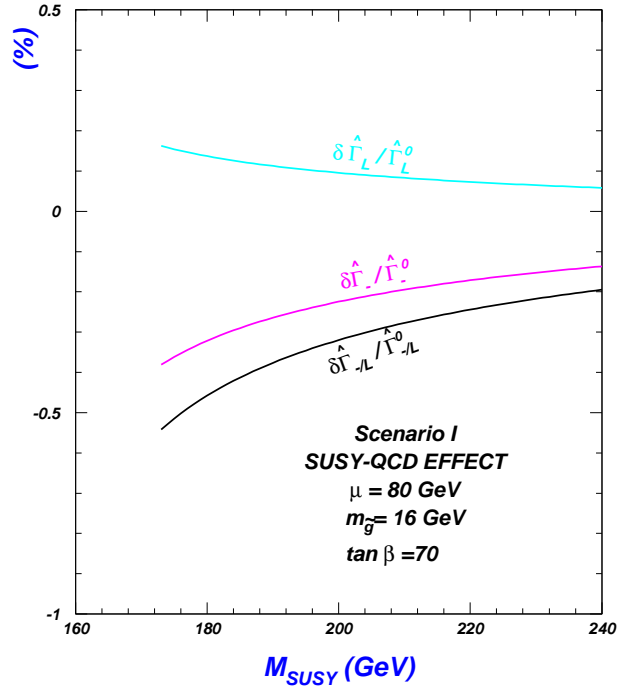


FIG. 10. SUSY-QCD correction to $\hat{\Gamma}_{-,L}$ and $\hat{\Gamma}_{-/L}$ versus M_{SUSY} in Scenario I.

Next we present results in Scenario II. As mentioned earlier, in Scenario II it is convenient to choose

$$m_{\tilde{b}_1}, m_{\tilde{t}_1}, m_{\tilde{t}_2}, \mu, A_b, \theta_b, \tan \beta, m_{\tilde{g}} \quad (14)$$

as input parameters. Our numerical studies show that the SUSY-QCD corrections are only sensitive to $m_{\tilde{t}_1}$ and $m_{\tilde{g}}$. So we fix $m_{\tilde{b}_1} = 5$ GeV, $m_{\tilde{t}_2} = 500$ GeV, $\mu = 80$ GeV, $A_b = 300$ GeV, $\tan\beta = 70$ and $\cos\theta_b = 0.38$ and plot the corrections in Figs. 11 and 12 for different gluino masses. Since in this scenario we assume a very light sbottom ($m_{\tilde{b}_1} = 5$ GeV), we do not consider the possibility of a very light gluino ($m_{\tilde{g}} = 16$ GeV) due to the R_b constraints [30]. From the figure we can see that for a $m_{\tilde{t}_1} = 100$ GeV and $m_{\tilde{g}} = 100$ GeV, SUSY-QCD corrections can reach -3% , comparable in magnitude with SUSY-EW corrections.

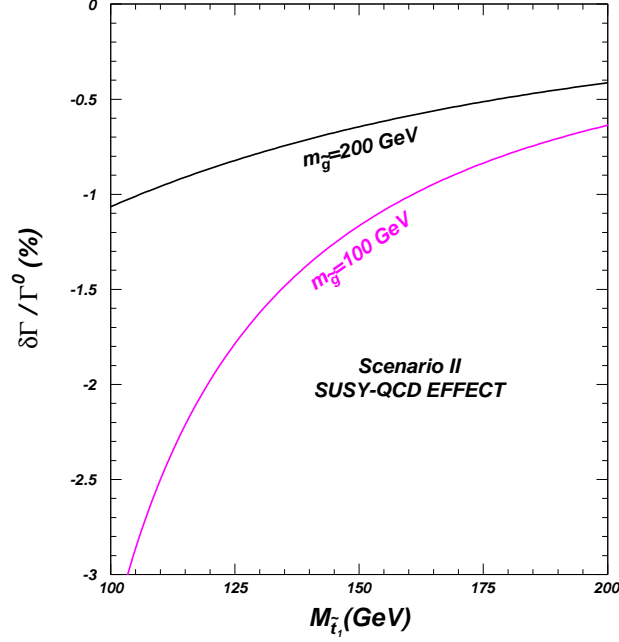


FIG. 11. SUSY-QCD corrections to Γ versus the lighter top-squark mass in Scenario II.

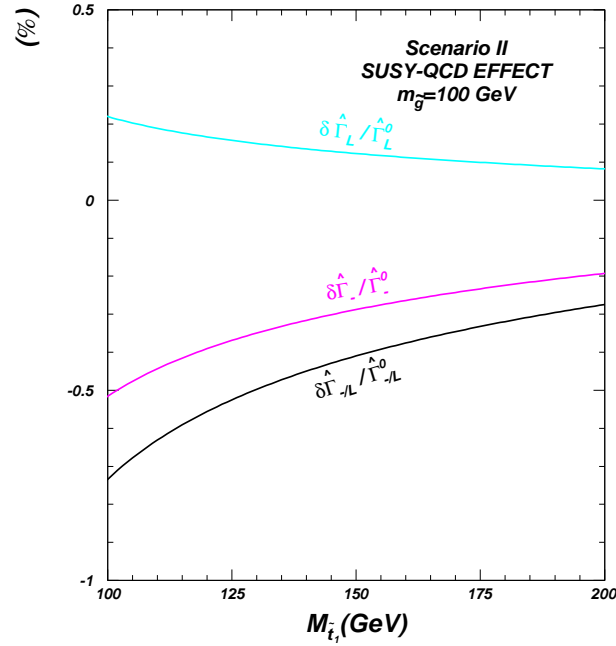


FIG. 12. SUSY-QCD corrections to $\hat{\Gamma}_{-,L}$ and $\hat{\Gamma}_{-/L}$ versus the lighter top-squark mass in Scenario II.

V. SUMMARY AND CONCLUSION

We investigated the one-loop SUSY-QCD and SUSY-EW corrections to the top quark decay into a b -quark and a longitudinal or transverse W -boson. The corrections are presented in terms of the longitudinal ratio $\Gamma(t \rightarrow W_L b)/\Gamma(t \rightarrow W b)$ and the transverse ratio $\Gamma(t \rightarrow W_{\perp} b)/\Gamma(t \rightarrow W b)$, and, in order to compare with the existing results in the literature, we also present the corrections to the total width $\Gamma(t \rightarrow W b)$. To find out the typical size of these corrections, we performed a scan in the typical allowed parameter space. Then, in order to decide if the corrections are exceptionally large in certain corners of parameter space, we considered some special scenarios (such as a very light sbottom or gluino). Our observations are:

- (1) In most of the parameter space, both SUSY-QCD and SUSY-EW corrections to the ratios are less than 1% in magnitude and they tend to have opposite signs. Only in some corners of parameter space can the corrections reach even a few percent.
- (2) The corrections to the total width $\Gamma(t \rightarrow W b)$ agree well with previous calculations for the SUSY-QCD part, but differ significantly from previous calculations for the SUSY-EW part. Unlike the previous studies, which showed a large SUSY-EW correction of more than 10% in magnitude for a large part of the parameter space, our SUSY-EW results are only a few percent, at most.

We conclude by remarking that these SUSY corrections, despite their smallness in size, should be taken into account in the future precision tests of the top quark decay $t \rightarrow W b$ to determine if SUSY is indeed the new physics chosen by Nature. (So far as we know, the corrections to tWb coupling in other kinds of new physics models are also very small [31].) However, from the viewpoint of probing SUSY through revealing its effects in the coupling tWb , the decay $t \rightarrow W b$ may not be the best channel. Some single top quark production channels proceeding through the tWb coupling may be complementary or even do better in this aspect. For example, SUSY effects in the tWb coupling may cause observable effects in single top quark production in hadron collisions [32], and the single top quark production via electron-photon collision at a future linear collider is also quite sensitive to anomalous tWb coupling [33].

ACKNOWLEDGMENT

This work is supported in part by the Chinese Natural Science Foundation and by the US Department of Energy, Division of High Energy Physics under grant No. DE-FG02-91-ER4086.

APPENDIX A: SUSY-EW LOOP RESULTS

In this appendix we first list the mass matrices of sfermions, charginos and neutralinos involved in our calculations, then write down the relevant interaction Lagrangian and finally present the explicit expressions of the SUSY-EW contributions from the loop diagrams shown in Fig.1.

1. Mass matrices of sfermions, charginos and neutralinos

Assuming no generation mixing for squarks in the soft-breaking terms, the mass-square matrices for up-type and down-type squarks in each generation are given respectively by [19]

$$M_{\tilde{u}}^2 = \begin{pmatrix} \tilde{M}_Q^2 + m_Z^2 \cos 2\beta (\frac{1}{2} - e_u \sin^2 \theta_W) + m_u^2 & m_u (A_u - \mu \cot \beta) \\ m_u (A_u - \mu \cot \beta) & \tilde{M}_U^2 + m_Z^2 \cos 2\beta e_u \sin^2 \theta_W + m_u^2 \end{pmatrix}, \quad (\text{A1})$$

$$M_{\tilde{d}}^2 = \begin{pmatrix} \tilde{M}_Q^2 - m_Z^2 \cos 2\beta (\frac{1}{2} + e_d \sin^2 \theta_W) + m_d^2 & m_d (A_d - \mu \tan \beta) \\ m_d (A_d - \mu \tan \beta) & \tilde{M}_D^2 + m_Z^2 \cos 2\beta e_d \sin^2 \theta_W + m_d^2 \end{pmatrix}, \quad (\text{A2})$$

where \tilde{M}_Q , \tilde{M}_U and \tilde{M}_D are soft-breaking mass terms for left-handed squark doublet, right-handed up and down squarks, respectively. A_u (A_d) is the coefficient of the trilinear term $H_2 \tilde{Q} \tilde{U}$ ($H_1 \tilde{Q} \tilde{D}$) in soft-breaking terms, and $\tan \beta = v_2/v_1$ is ratio of the vacuum expectation values of the two Higgs doublets.

For the first two generation squarks, the left-right mixings can be neglected due to the smallness of relevant quark masses and thus the weak-eigenstates are mass-eigenstates. Then from Eqs.(A1,A2) we get the relation between the left-handed up-type squark mass $M_{\tilde{u}_L}$ and the left-handed down-type squark mass $M_{\tilde{d}_L}$

$$M_{uL}^2 = M_{dL}^2 + m_Z^2 \cos 2\beta (1 - \sin^2 \theta_W) + m_u^2 - m_d^2. \quad (\text{A3})$$

For the third generation squarks, the left-right mixings cannot be neglected and the mass-eigenstates $\tilde{q}_{1,2}$ ($q = t, b$) are related to the weak-eigenstates $\tilde{q}_{L,R}$ by an unitary rotation R

$$\begin{pmatrix} \tilde{q}_1 \\ \tilde{q}_2 \end{pmatrix} = R \begin{pmatrix} \tilde{q}_L \\ \tilde{q}_R \end{pmatrix} \equiv \begin{pmatrix} \cos \theta_q & \sin \theta_q \\ -\sin \theta_q & \cos \theta_q \end{pmatrix} \begin{pmatrix} \tilde{q}_L \\ \tilde{q}_R \end{pmatrix}, \quad (\text{A4})$$

where θ_q is the so-called mixing angle between \tilde{q}_L and \tilde{q}_R .

The mass-square matrices in Eqs.(A1, A2) can be alternatively expressed by the squark masses and mixing angle as

$$M_{\tilde{q}}^2 = \begin{pmatrix} \cos^2 \theta_q m_{\tilde{q}_1}^2 + \sin^2 \theta_q m_{\tilde{q}_2}^2 & \sin \theta_q \cos \theta_q (m_{\tilde{q}_1}^2 - m_{\tilde{q}_2}^2) \\ \sin \theta_q \cos \theta_q (m_{\tilde{q}_1}^2 - m_{\tilde{q}_2}^2) & \sin^2 \theta_q m_{\tilde{q}_1}^2 + \cos^2 \theta_q m_{\tilde{q}_2}^2 \end{pmatrix}. \quad (\text{A5})$$

By comparing Eq.(A5) with Eqs.(A1, A2), one can obtain the relationship between the two set of input parameters in squark sector, $(m_{\tilde{q}_1}, m_{\tilde{q}_2}, \theta_q)$ and $(\tilde{M}_Q, \tilde{M}_U, \tilde{M}_D, A_{t,b}, \mu)$. The mass matrices for sleptons take the similar forms as squarks. But due to the smallness of lepton masses, the left-right mixings can be neglected for the three generations.

The mass matrices of charginos and neutralinos are also involved in our calculations. The chargino mass matrix can be diagonalized by two unitary matrices U and V

$$U^* \begin{pmatrix} \tilde{M}_2 & m_W \sqrt{2} \sin \beta \\ m_W \sqrt{2} \cos \beta & \mu \end{pmatrix} V^{-1} = \text{diag} \{ m_{\tilde{\chi}_i^+} \} \quad (i = 1, 2). \quad (\text{A6})$$

The neutralino mass matrix is given by

$$Y = \begin{pmatrix} \tilde{M}_1 & 0 & -m_Z \sin \theta_W \cos \beta & m_Z \sin \theta_W \sin \beta \\ 0 & \tilde{M}_2 & m_Z \cos \theta_W \cos \beta & -m_Z \cos \theta_W \sin \beta \\ -m_Z \sin \theta_W \cos \beta & m_Z \cos \theta_W \cos \beta & 0 & -\mu \\ m_Z \sin \theta_W \sin \beta & -m_Z \cos \theta_W \sin \beta & -\mu & 0 \end{pmatrix}, \quad (\text{A7})$$

and it can be diagonalized by an unitary matrix N

$$N^* Y N^{-1} = \text{diag} \{ m_{\tilde{\chi}_j^0} \} \quad (j = 1, 2, 3, 4). \quad (\text{A8})$$

In the above expressions \tilde{M}_1 and \tilde{M}_2 are respectively the soft-breaking $U(1)$ and $SU(2)$ gaugino masses. $m_{\tilde{\chi}_i^+}$ and $m_{\tilde{\chi}_j^0}$ are the masses of charginos and neutralinos, respectively. One point we want to remind is U , V and N defined in Eq.(A6, A8) are not unique and one should choose U , V and N so that all the masses of charginos and neutralinos are positive.

2. Interaction Lagrangian

The interaction Lagrangian relevant for our calculations is given by

$$\begin{aligned} \mathcal{L} = & -\frac{g}{2} \left\{ \tilde{t}_\alpha^* \tilde{\chi}_i^- (A_{\alpha i}^t - B_{\alpha i}^t \gamma_5) b + \tilde{b}_\beta^* \tilde{\chi}_i^+ (A_{\beta i}^b - B_{\beta i}^b \gamma_5) t + \tilde{t}_\alpha^* \tilde{\chi}_j^0 (A_{\alpha j}^{t(0)} - B_{\alpha j}^{t(0)} \gamma_5) t + \tilde{b}_\beta^* \tilde{\chi}_j^0 (A_{\beta j}^{b(0)} - B_{\beta j}^{b(0)} \gamma_5) b \right\} \\ & - \frac{g}{\sqrt{2}} R_{\alpha 1}^t R_{\beta 1}^b \tilde{t}_\alpha^* \overleftrightarrow{\partial}^\mu \tilde{b}_\beta W_\mu^+ + g \tilde{\chi}_j^0 \gamma^\mu (O_{ij}^L P_L + O_{ij}^R P_R) \tilde{\chi}_i^- W_\mu^+ \\ & + \frac{g^2}{2} (R_{\alpha 1}^t R_{\alpha 2}^t \tilde{t}_\alpha^* \tilde{t}_{\alpha 2} + R_{\beta 1}^b R_{\beta 2}^b \tilde{b}_\beta^* \tilde{b}_{\beta 2}) W_\mu^- W^{\mu+} + h.c., \end{aligned} \quad (\text{A9})$$

where the sum over repeated indices is implied, and

$$A_{\alpha i}^t = R_{\alpha 1}^t (V_{i1}^* - \lambda_b U_{i2}) - R_{\alpha 2}^t \lambda_t V_{i2}^*, \quad (\text{A10})$$

$$B_{\alpha i}^t = R_{\alpha 1}^t (V_{i1}^* + \lambda_b U_{i2}) - R_{\alpha 2}^t \lambda_t V_{i2}^*, \quad (\text{A11})$$

$$A_{\beta i}^b = R_{\beta 1}^b (U_{i1}^* - \lambda_t V_{i2}) - R_{\beta 2}^b \lambda_b U_{i2}^*, \quad (\text{A12})$$

$$B_{\beta i}^b = R_{\beta 1}^b (U_{i1}^* + \lambda_t V_{i2}) - R_{\beta 2}^b \lambda_b U_{i2}^* , \quad (\text{A13})$$

$$A_{\alpha j}^{t(0)} = R_{\alpha 1}^t (\lambda_t N_{j4} + \sqrt{2}(\frac{1}{6} N_{j1}^* \tan \theta_W + \frac{1}{2} N_{j2}^*)) + R_{\alpha 2}^t (\lambda_t N_{j4}^* - \sqrt{2} \frac{2}{3} N_{j1} \tan \theta_W) , \quad (\text{A14})$$

$$B_{\alpha j}^{(0)} = R_{\alpha 1}^t (-\lambda_t N_{j4} + \sqrt{2}(\frac{1}{6} N_{j1}^* \tan \theta_W + \frac{1}{2} N_{j2}^*)) + R_{\alpha 2}^t (\lambda_t N_{j4}^* + \sqrt{2} \frac{2}{3} N_{j1} \tan \theta_W) , \quad (\text{A15})$$

$$A_{\beta j}^{b(0)} = R_{\beta 1}^b (\lambda_b N_{j3} + \sqrt{2}(\frac{1}{6} N_{j1}^* \tan \theta_W - \frac{1}{2} N_{j2}^*)) + R_{\beta 2}^b (\lambda_b N_{j3}^* + \frac{\sqrt{2}}{3} N_{j1} \tan \theta_W) , \quad (\text{A16})$$

$$B_{\beta j}^{b(0)} = R_{\beta 1}^b (-\lambda_b N_{j3} + \sqrt{2}(\frac{1}{6} N_{j1}^* \tan \theta_W - \frac{1}{2} N_{j2}^*)) + R_{\beta 2}^b (\lambda_b N_{j3}^* - \frac{\sqrt{2}}{3} N_{j1} \tan \theta_W) , \quad (\text{A17})$$

$$O_{ij}^L = -\frac{1}{\sqrt{2}} N_{j4} V_{i2}^* + N_{j2} V_{i1}^* , \quad (\text{A18})$$

$$O_{ij}^R = \frac{1}{\sqrt{2}} N_{j3}^* U_{i2} + N_{j2}^* U_{i1} . \quad (\text{A19})$$

Here $\lambda_t = \frac{m_t}{\sqrt{2} m_W \sin \beta}$ and $\lambda_b = \frac{m_b}{\sqrt{2} m_W \cos \beta}$. Note that the Lagrangian used in Ref. [13] takes a different form from ours since Ref. [13] used unusual notations for chargino and neutralino mass matrices, but the resulted interactions are the same. (Here 'unusual' means different from the notations of Ref. [19].)

3. Analytic results of SUSY-EW loops

To compare our results with those in Ref. [13], we present our results in the same way as in Ref. [13]. First, from matrices in Eqs.(A10-A19) we define the following matrices

$$A_{\pm}^t = A^t \pm B^t , \quad A_{\pm}^{t(0)} = A^{t(0)} \pm B^{t(0)} , \quad (\text{A20})$$

$$A_{\pm}^b = A^b \pm B^b , \quad A_{\pm}^{b(0)} = A^{b(0)} \pm B^{b(0)} , \quad (\text{A21})$$

and construct the combinations as

$$A^{(1)} = -A_+^{t*} O^R A_-^{t(0)} , \quad E^{(1)} = -A_-^{t*} O^R A_-^{t(0)} , \quad (\text{A22})$$

$$B^{(1)} = -A_+^{t*} O^R A_+^{t(0)} , \quad F^{(1)} = -A_-^{t*} O^R A_+^{t(0)} , \quad (\text{A23})$$

$$C^{(1)} = -A_+^{t*} O^L A_-^{t(0)} , \quad G^{(1)} = -A_-^{t*} O^L A_-^{t(0)} , \quad (\text{A24})$$

$$D^{(1)} = -A_+^{t*} O^L A_+^{t(0)} , \quad H^{(1)} = -A_-^{t*} O^L A_+^{t(0)} , \quad (\text{A25})$$

$$A^{(2)} = -R_{\alpha 1}^t R_{\beta 1}^b A_+^{b(0)*} A_-^{t(0)} , \quad C^{(2)} = -R_{\alpha 1}^t R_{\beta 1}^b A_-^{b(0)*} A_-^{t(0)} , \quad (\text{A26})$$

$$B^{(2)} = -R_{\alpha 1}^t R_{\beta 1}^b A_+^{b(0)*} A_+^{t(0)} , \quad D^{(2)} = -R_{\alpha 1}^t R_{\beta 1}^b A_-^{b(0)*} A_+^{t(0)} , \quad (\text{A27})$$

$$A^{(3)} = A_+^{b(0)*} O^L A_-^b , \quad E^{(3)} = A_-^{b(0)*} O^L A_-^b , \quad (\text{A28})$$

$$B^{(3)} = A_+^{b(0)*} O^L A_+^b , \quad F^{(3)} = A_-^{b(0)*} O^L A_+^b , \quad (\text{A29})$$

$$C^{(3)} = A_+^{b(0)*} O^R A_-^b , \quad G^{(3)} = A_-^{b(0)*} O^R A_-^b , \quad (\text{A30})$$

$$D^{(3)} = A_+^{b(0)*} O^R A_+^b , \quad H^{(3)} = A_-^{b(0)*} O^R A_+^b . \quad (\text{A31})$$

Then the contributions of vertex loop diagrams (a,b,c) in Fig.1 to the form factors $F_{L,R}$ and $H_{L,R}$ are given as follows.

- **Diagram (a):**

$$F_L^{(a)} = \frac{\sqrt{2} g^2}{4 V_{tb}} \frac{1}{16 \pi^2} \left\{ -\frac{1}{2} D^{(1)} (-1 + 4 C_{24}) + m_{\tilde{\chi}_j^0} m_{\tilde{\chi}_i^-} B^{(1)} C_0 - m_{\tilde{\chi}_j^0} m_t C^{(1)} (C_{11} - C_{12}) \right. \\ \left. + m_{\tilde{\chi}_i^-} m_t A^{(1)} (C_0 + C_{11} - C_{12}) - m_t^2 D^{(1)} (C_{11} - C_{12} + C_{21} - C_{23}) - m_W^2 D^{(1)} (C_{22} - C_{23}) \right\} , \quad (\text{A32})$$

$$F_R^{(a)} = \frac{\sqrt{2} g^2}{4 V_{tb}} \frac{1}{16 \pi^2} \left\{ -\frac{1}{2} E^{(1)} (-1 + 4 C_{24}) + m_{\tilde{\chi}_j^0} m_{\tilde{\chi}_i^-} G^{(1)} C_0 - m_{\tilde{\chi}_j^0} m_t F^{(1)} (C_{11} - C_{12}) \right\}$$

$$+m_{\tilde{\chi}_i^-} m_t H^{(1)}(C_0 + C_{11} - C_{12}) - m_t^2 E^{(1)}(C_{11} - C_{12} + C_{21} - C_{23}) - m_W^2 E^{(1)}(C_{22} - C_{23}) \Big\} , \quad (\text{A33})$$

$$H_L^{(a)} = \frac{\sqrt{2}g^2}{4V_{tb}} \frac{1}{16\pi^2} \left\{ 2m_{\tilde{\chi}_j^0} F^{(1)}(C_{11} - C_{12}) + 2m_{\tilde{\chi}_i^-} H^{(1)}C_{12} + 2m_t E^{(1)}(C_{11} - C_{12} + C_{21} - C_{23}) \right\} , \quad (\text{A34})$$

$$H_R^{(a)} = \frac{\sqrt{2}g^2}{4V_{tb}} \frac{1}{16\pi^2} \left\{ 2m_{\tilde{\chi}_j^0} C^{(1)}(C_{11} - C_{12}) + 2m_{\tilde{\chi}_i^-} A^{(1)}C_{12} + 2m_t D^{(1)}(C_{11} - C_{12} + C_{21} - C_{23}) \right\} , \quad (\text{A35})$$

where the functions C_0 and C_{nm} are 3-point Feynman integrals defined in Ref. [34] with functional dependence $C_0, C_{nm}(-p_t, p_W, m_{\tilde{t}_\alpha}, m_{\tilde{\chi}_j^0}, m_{\tilde{\chi}_i^-})$.

• **Diagram (b):**

$$F_L^{(b)} = \frac{g^2}{2V_{tb}} \frac{1}{16\pi^2} \left\{ -B^{(2)}C_{24} \right\} , \quad (\text{A36})$$

$$F_R^{(b)} = \frac{g^2}{2V_{tb}} \frac{1}{16\pi^2} \left\{ -C^{(2)}C_{24} \right\} , \quad (\text{A37})$$

$$H_L^{(b)} = \frac{g^2}{2V_{tb}} \frac{1}{16\pi^2} \left\{ m_{\tilde{\chi}_j^0} D^{(2)}(C_0 + C_{11}) + m_t C^{(2)}(C_{12} - C_{11} - C_{21} + C_{23}) \right\} , \quad (\text{A38})$$

$$H_R^{(a)} = \frac{g^2}{2V_{tb}} \frac{1}{16\pi^2} \left\{ m_{\tilde{\chi}_j^0} A^{(2)}(C_0 + C_{11}) + m_t B^{(2)}(C_{12} - C_{11} - C_{21} + C_{23}) \right\} , \quad (\text{A39})$$

with the Feynman integrals $C_0, C_{nm}(-p_t, p_W, m_{\tilde{\chi}_j^0}, m_{\tilde{t}_\alpha}, m_{\tilde{b}_\beta})$.

• **Diagram (c) :**

$F_{L,R}^{(c)}$ and $H_{L,R}^{(c)}$ can be obtained from the corresponding $F_{L,R}^{(a)}$ and $H_{L,R}^{(a)}$ with the replacements:

$$\begin{aligned} m_{\tilde{t}_\alpha} &\rightarrow m_{\tilde{b}_\beta} , & m_{\tilde{\chi}_j^0} &\leftrightarrow m_{\tilde{\chi}_i^-} , & A^{(1)} &\rightarrow A^{(3)} , & B^{(1)} &\rightarrow B^{(3)} , \\ C^{(1)} &\rightarrow C^{(3)} , & D^{(1)} &\rightarrow D^{(3)} , & E^{(1)} &\rightarrow E^{(3)} , & H^{(1)} &\rightarrow H^{(3)} . \end{aligned} \quad (\text{A40})$$

For the self-energy loop diagrams in (d,e) of Fig. 1, we only present the corresponding forms of $\Sigma_{\tilde{\chi}^-}$ (from chargino loops) and of $\Sigma_{\tilde{\chi}^0}$ (from neutralino loops). The renormalization constants $\delta Z_{t,b}^L$ can be obtained straitforwardly by using Eqs.(4, 5). The results are given by

• **Diagram (d) :**

$$\begin{aligned} \Sigma_{\tilde{\chi}^-}^t(p) &= \frac{g^2}{4} \frac{1}{16\pi^2} \left\{ (|A_+^b|^2 \not{p}P_L + |A_-^b|^2 \not{p}P_R)B_1(p, m_{\tilde{\chi}_i^-}, m_{\tilde{b}_\beta}) \right. \\ &\quad \left. - m_{\tilde{\chi}_i^-} (A_-^{b*} A_+^b P_L + A_+^{b*} A_-^b P_R)B_0(p, m_{\tilde{\chi}_i^-}, m_{\tilde{b}_\beta}) \right\} , \end{aligned} \quad (\text{A41})$$

$$\begin{aligned} \Sigma_{\tilde{\chi}^0}^t(p) &= \frac{g^2}{4} \frac{1}{16\pi^2} \left\{ (|A_+^{t(0)}|^2 \not{p}P_L + |A_-^{t(0)}|^2 \not{p}P_R)B_1(p, m_{\tilde{\chi}_j^0}, m_{\tilde{t}_\alpha}) \right. \\ &\quad \left. - m_{\tilde{\chi}_j^0} (A_-^{t(0)*} A_+^{t(0)} P_L + A_+^{t(0)*} A_-^{t(0)} P_R)B_0(p, m_{\tilde{\chi}_j^0}, m_{\tilde{t}_\alpha}) \right\} . \end{aligned} \quad (\text{A42})$$

• **Diagram (e) :**

$$\begin{aligned} \Sigma_{\tilde{\chi}^-}^b(p) &= \frac{g^2}{4} \frac{1}{16\pi^2} \left\{ (|A_+^t|^2 \not{p}P_L + |A_-^t|^2 \not{p}P_R)B_1(p, m_{\tilde{\chi}_i^-}, m_{\tilde{t}_\alpha}) \right. \\ &\quad \left. - m_{\tilde{\chi}_i^-} (A_-^{t*} A_+^t P_L + A_+^{t*} A_-^t P_R)B_0(p, m_{\tilde{\chi}_i^-}, m_{\tilde{t}_\alpha}) \right\} , \end{aligned} \quad (\text{A43})$$

$$\begin{aligned} \Sigma_{\tilde{\chi}^0}^b(p) &= \frac{g^2}{4} \frac{1}{16\pi^2} \left\{ (|A_+^{b(0)}|^2 \not{p}P_L + |A_-^{b(0)}|^2 \not{p}P_R)B_1(p, m_{\tilde{\chi}_j^0}, m_{\tilde{b}_\beta}) \right. \\ &\quad \left. - m_{\tilde{\chi}_j^0} (A_-^{b(0)*} A_+^{b(0)} P_L + A_+^{b(0)*} A_-^{b(0)} P_R)B_0(p, m_{\tilde{\chi}_j^0}, m_{\tilde{b}_\beta}) \right\} . \end{aligned} \quad (\text{A44})$$

Comparing our above results with those in [13], we found that our slef-energy loop results essentially agree with those of [13], but our vertex loop results disagree with those of [13]. The analytic results of [13] seem to have some explicit errors, e.g., the UV divergence in F_L seems unable to be canceled, terms like $m_t C_0$ should not appear in $H_{L,R}$ and G_2 and G_3 should be interchanged.

APPENDIX B: EXPLANATION OF THRESHOLD BEHAVIORS

The two-point loop functions $B'_{0,1}(p, m_1, m_2)|_{p^2=m_2^2}$ enter our results via δZ_t^L . In order to explain the threshold behavior in Figs.(2, 4, 6), we study the behavior of $B'_{0,1}(m_0, m_1, m_2)$ near the threshold point $m_0 = m_1 + m_2$. We take B'_0 as an example and the behavior of B'_1 is similar.

For fixed m_0 and m_2 , $B'_0(m_0, m_1, m_2)$ as a function of m_1 can be expressed as

$$B'_0 = \int_0^1 \frac{x - x^2}{m_0^2 x^2 - (m_0^2 + m_1^2 - m_2^2)x + m_1^2} dx$$

$$= \begin{cases} \frac{1}{m_0^2} \int_0^1 \frac{x-x^2}{(x-a)^2 - b^2} dx & \text{for } m_1 < m_0 - m_2, \\ \frac{1}{m_0^2} \int_0^1 \frac{x-x^2}{(x-a)^2} dx & \text{for } m_1 = m_0 - m_2, \\ \frac{1}{m_0^2} \int_0^1 \frac{x-x^2}{(x-a)^2 + b^2} dx & \text{for } m_1 > m_0 - m_2, \end{cases} \quad (\text{B1})$$

where

$$a = \frac{m_0^2 + m_1^2 - m_2^2}{2m_0^2}, \quad (\text{B2})$$

$$b = \frac{1}{2m_0^2} \sqrt{|(m_0 + m_1 + m_2)(m_0 + m_1 - m_2)(m_0 - m_1 + m_2)(m_0 - m_1 - m_2)|}. \quad (\text{B3})$$

From Eq.(B1), one may infer that, in regions below threshold ($m_1 < m_0 - m_2$) or above threshold ($m_1 > m_0 - m_2$), B'_0 is an continuous function of m_1 . At the threshold point ($m_1 = m_0 - m_2$), B'_0 is divergent due to the fact $0 < a < 1$. (In some calculation programs, such as LoopTools [35] used in our calculations, an imaginary part is added to the propagators in the loops to avoid the divergence at the threshold point.)

In the limit $m_1 \rightarrow m_0 - m_2$ from left-side (i.e. $m_1 < m_0 - m_2$), $B'_0 \rightarrow -2 + (1 - 2a) \ln [(1 - a)/a]$ which is a finite value and corresponds to the top points in Figs.(2, 4, 6). But in the limit $m_1 \rightarrow m_0 - m_2$ from right-side (i.e. $m_1 > m_0 - m_2$), $B'_0 \rightarrow \infty$ which corresponds to the bottom point in Figs.(2, 4, 6). Since these bottom points tend to be negatively very large, the perturbative calculation is not reliable at these points.

- [1] For example, top-pair production at hadron collisions are quite sensitive to new physics. For comprehensive model-independent analyses, see, e.g., C. T. Hill and S. J. Parke, Phys. Rev. D **49**, 4454 (1994); K. Whisnant, et al., Phys. Rev. D **56**, 467 (1997); K. Hikasa, et al., Phys. Rev. D **58**, 114003 (1998).
- [2] For recent reviews on top quark, see, e.g., C. T. Hill and E. Simmons, hep-ph/0203079; C.-P. Yuan, hep-ph/0203088; E. Simmons, hep-ph/0211335; S. Willenbrock, hep-ph/0211067; D. Chakraborty, J. Konigsberg, D. Rainwater, hep-ph/0303092.
- [3] See, e.g., A. Datta, et al., Phys. Rev. D **56**, 3107 (1997); R. J. Oakes, et al., Phys. Rev. D **57**, 534 (1998); K. Hikasa, J. M. Yang, B.-L. Young, Phys. Rev. D **60**, 114041 (1999); C. Balazs, H.-J. He, C.-P. Yuan, Phys. Rev. D **60**, 114001 (1999); H.-J. He, C.P. Yuan, Phys. Rev. Lett. **83**, 28 (1999); G. Burdman, Phys. Rev. Lett. **83**, 2888 (1999); P. Chiappetta, et al., Phys. Rev. D **61**, 115008 (2000); J. Cao, Z. Xiong and J. M. Yang, Nucl. Phys. B **651**, 87 (2003); Phys. Rev. D **67**, 071701 (2003).
- [4] See, e.g., M. Hosch, et al., Phys. Rev. D **58**, 034002 (1998); S. Mrenna and C.P. Yuan, Phys. Lett. B **367**, 188 (1996). C. S. Li, R. J. Oakes and J. M. Yang, Phys. Rev. D **49**, 293 (1994); J. L. Lopez, D. V. Nanopoulos and R. Rangarajan, Phys. Rev. D **56**, 3100 (1997); G. Eilam, et al., Phys. Lett. B **510**, 227 (2001); K.J. Abraham, et al., Phys. Lett. B **514**, 72 (2001); Phys. Rev. D **63**, 034011 (2001); T. Han and J. Hewett, Phys. Rev. D **60**, 074015 (1999); F. del Aguila, J. A. Aguilar-Saavedra, R. Miquel, Phys. Rev. Lett. **82**, 1628 (1999); X. L. Wang et al., Phys. Rev. D **50**, 5781 (1994).
- [5] See, e.g., C. A. Nelson, *et al.*, Phys. Rev. D **56**, 5928(1997); Phys. Rev. D **57**, 5923 (1998); C. A. Nelson and A. M. Cohen, Euro. Phys. J. C **8**, 393 (1999); C. A. Nelson and L. J. Adler, Euro. Phys. J. C **17**, 399 (2000); C. A. Nelson, Euro. Phys. J. C **19**, 323 (2001); F. del Aguila and J. A. Aguilar-Saavedra, Phys. Rev. D **67**, 014009 (2003).
- [6] Y. Bigi, *et al.*, Phys. Lett. B **181**, 157 (1986).
- [7] CDF collaboration, T. Affolder, *et al.*, Phys. Rev. Lett. **84**, 216 (2000).
- [8] S. Willenbrock, Rev. Mod. Phys. **72**, 1141(2000).
- [9] M. Fischer, S. Groote, J. G. Korner and M. C. Mauser, Phys. Rev. D **63**, 031501 (2001); Phys. Rev. D **65**, 054036 (2002).

- [10] M. Fischer, S. Groote, J. G. Korner and M. C. Mauser, Phys. Rev. D **67**, 091501 (2003).
- [11] J. M. Yang and C. S. Li, Phys. Lett. B **320**, 117 (1994).
- [12] C. S. Li, J. M. Yang and B. Q. Hu, Phys. Rev. D **48**, 5425 (1993).
- [13] D. Garcia, R. A. Jimenez, J. SOLA and W. Hollik, Nucl. Phys. B **427**, 53 (1994).
- [14] A. Dabelstein, W. Hollik, C. Juenger, R. A. Jimenez and J. Sola, Nucl. Phys. B **454**, 75 (1995).
- [15] A. Brandenburg and M. Maniatis, Phys. Lett. B **545**, 139 (2002).
- [16] B. Grzadkowski and W. Hollik, Nucl. Phys. B **384**, 101 (1992).
- [17] M. Bohm, H. Spiesberger and W. Hollik, Fortsch. Phys. **34**, 687 (1986); W. Hollik, Fortsch. Phys. **38**, 165(1990).
- [18] A. Denner, Fortsch. Phys. **41**, 307 (1993).
- [19] H. E. Haber and G. L. Kane, Phys. Rept. **117**, 75 (1985); J. F. Gunion and H. E. Haber, Nucl. Phys. B **272**, 1 (1986).
- [20] See, e.g., J. A. Grifols and J. Sola, Nucl. Phys. B **253**, 47 (1985); D. Garcia and J. Sola, Mod. Phys. Lett. A **9**, 211 (1994); R. Hempfling and B. A. Kniehl, Z. Phys. C **59**, 263 (1993).
- [21] P. H. Chankowski, *et al.*, Nucl. Phys. B **417**, 101 (1994).
- [22] J. Fleischer and F. Jegerlehner, Phys. Rev. D **23**, 2001 (1981); Nucl. Phys. B **216**, 469 (1983); A. Dabelstein and W. Hollik, Z. Phys. C **53**, 507 (1992).
- [23] H. P. Nilles, Phys. Rept. **110**, 1 (1984); A. B. Lahanas and D. V. Nanopoulos, Phys. Rept. **145**, 1 (1987).
- [24] H. N Brown, *et al.*, Mu g-2 Collaboration, Phys. Rev. Lett. **86**, 2227 (2001).
- [25] Particle Physics Group. Euro. Phys. J. C **15**, 274 (2000).
- [26] S. Heinemeyer, W. Hollik and G. Weiglein, Comput. Phys. Commun. **124**, 76 (2000).
- [27] R. Barate *et al.*, ALEPH Collaboration, Phys. Lett. B **499**, 53 (2001); LEP Higgs Working Group, hep-ex/0107029; hep-ex/0107030; U. Schwickerath, hep-ph/0205126.
- [28] M. Carena, S. Heinemeyer, C. E. Wagner and G. Weiglein, Phys. Rev. Lett. **86**, 4463 (2001).
- [29] E. L. Berger, *et al.*, Phys. Rev. Lett. **86**, 4231 (2001).
- [30] J. Cao, Z. Xiong and J. M. Yang, Phys. Rev. Lett. **88**, 111802 (2002); G. C. Cho, Phys. Rev. Lett. **89**, 091801 (2002); K. Cheung and W. Y. Keung, Phys. Rev. Lett. **89**, 221801 (2002); Z. Luo and J. L. Rosner, hep-ph/0306022; R. Malhotra, hep-ph/0306183.
- [31] See, e.g., N. Mahajan, hep-ph/0304235.
- [32] C. S. Li, *et al.*, Phys. Rev. D **57**, 2009 (1998); Phys. Lett. B **98**, 298 (1997); Phys. Rev. D **55**, 5780 (1997);
- [33] J. J. Cao *et al.*, Phys. Rev. D **58**, 094004 (1998); E. Boos, *et al.*, Euro. Phys. J. C **21**, 81 (2001).
- [34] A. Axelrod, Nucl. Phys. B **209**, 349 (1982).
- [35] T. Hahn, Nucl. Phys. Proc. Suppl. **89**, 231 (2000); Acta Phys. Polon. **B30**, 3469 (1999).